Skeletal Radiol (2007) 36:1163–1169
DOI 10.1007/s00256-007-0374-7

SCIENTIFIC ARTICLE

Four-dimensional computed tomographic imaging in the wrist: proof of feasibility in a cadaveric model

Shian-Chao Tay · Andrew N. Primak · Joel G. Fletcher · Bernhard Schmidt · Kimberly K. Amrami · Richard A. Berger · Cynthia H. McCollough

Received: 14 May 2007 / Revised: 8 August 2007 / Accepted: 12 August 2007 / Published online: 6 September 2007

Abstract
Objective High-resolution real-time three-dimensional (3D) imaging of the moving wrist may provide novel insights into the pathophysiology of joint instability. The purpose of this work was to assess the feasibility of using retrospectively gated spiral computed tomography (CT) to perform four-dimensional (4D) imaging of the moving wrist joint.
Materials and methods A cadaver forearm from below the elbow was mounted on a motion simulator which performed radioulnar deviation of the wrist at 30 cycles per minute. An electronic trigger from the simulator provided the "electrocardiogram" (ECG) signal required for gated reconstructions. Four-dimensional and 3D images were compared by a blinded observer for image quality and presence of artifacts.
Results Image quality of 4D images was found to be excellent at the extremes of radial and ulnar deviation (end-motion phases). Some artifacts were seen in mid-motion phases.
Conclusion 4D CT musculoskeletal imaging is feasible. Four-dimensional CT may allow clinicians to assess functional (dynamic) instabilities of the wrist joint.

Keywords Four-dimensional wrist imaging · Dynamic carpal instabilities · Retrospectively gated spiral computed tomography · Dynamic real-time musculoskeletal imaging · Multi-detector CT

S.-C. Tay · R. A. Berger
Orthopedics Biomechanics Laboratory,
Mayo Clinic College of Medicine,
Rochester, MN, USA

A. N. Primak · J. G. Fletcher · K. K. Amrami · C. H. McCollough (✉)
Department of Radiology, Mayo Clinic College of Medicine,
200 First Street SW,
Rochester, MN 55905, USA
e-mail: mccollough.cynthia@mayo.edu

J. G. Fletcher · C. H. McCollough
CT Innovation Center, Mayo Clinic College of Medicine,
Rochester, MN, USA

B. Schmidt
Siemens Medical Solutions,
Forchheim, Germany

Introduction

High-resolution multi-detector row electrocardiogram (ECG)-gated computed tomography (CT) has enabled physicians to produce images of the beating heart for the analysis of myocardial wall function, cardiac valve function, and coronary artery stenosis [1–6]. ECG-gated CT has also been used for non-cardiac applications, such as four-dimensional (4D) imaging of pulmonary lesions [7–10].

A non-cardiac, non-thoracic application of gated CT imaging may lie in the field of musculoskeletal (MSK) imaging. Four-dimensional MSK imaging of the joint (i.e., real-time imaging during joint motion) may provide novel insights into the pathophysiology of joint instability. Some investigators have shown that a hysteresis effect occurs during joint motion [11, 12]. Hysteresis is defined as retardation of the effect when the forces acting upon a system are changed. A well-known hysteresis effect occurs during breathing, when there is a difference in the pressure–volume curve for lung inflation and deflation [13]. The carpal bones of the wrist joint demonstrate hysteresis that is dependent on the direction of wrist motion. For instance, the amount that the scaphoid or lunate bone flexes at a particular wrist position differs, depending on the direction

the wrist was moved to reach that position. In this case, the hysteresis can be described as the difference in the path of carpal bone motion [11, 12].

Instabilities of the wrist joint are a common cause of wrist pain. Such instabilities are classified as static or dynamic [14]. Static instabilities can be diagnosed on routine radiographs or conventional CT scans through abnormal carpal angles or carpal alignment. On the other hand, dynamic instabilities do not demonstrate any abnormalities on routine radiographic examinations, although these patients continue to have disabling wrist pain and inconsistent findings on clinical examination [15]. As a result, the delay in diagnoses may lead to poor clinical outcomes. In contrast, early detection of functional joint abnormalities may allow physicians to intervene with reconstructive surgical options to restore normal function before the onset of arthritis or static deformities[16–21]. This will result in better functional outcomes than joint arthroplasty or joint fusions, which are considered salvage procedures. Furthermore, it is suggested that the diagnosis of dynamic instabilities may rest on the ability of the physician to detect abnormal hysteresis during continuous joint motion [11]. Clearly, 4D imaging is the logical means to detect such dynamic joint instabilities [22].

The wrist is an ideal candidate for 4D MSK imaging using retrospectively-gated CT. One reason is that the wrist is of great clinical and research interest as a result of its complex structure [11, 23–27]. A second reason is that the individual carpal bones within the wrist do not undergo large displacements during the full range of motion. Finally, as mentioned, there is currently no objective means to diagnose and quantify dynamic carpal instabilities, particularly those of the scaphoid [14].

In 4D cardiac imaging, the heart rate, which is under involuntary autonomic control, is typically the limiting factor to image quality [28]. However, in 4D MSK imaging, the frequency and velocity of joint motion is largely under a person's volitional control. As a result of this volitional control, extremely slow motion frequencies can be used, suggesting the possibility of our imaging slow and periodic joint motion using retrospectively gated CT techniques. Work with phantoms has demonstrated the feasibility of this approach [29].

The purpose of this work was to assess the feasibility of using retrospectively gated spiral CT to image wrist joint motion in a mechanically controlled moving cadaveric specimen.

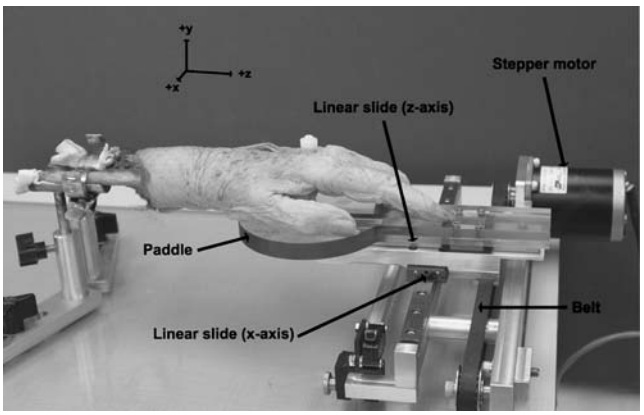

Fig. 1 The cadaveric wrist mounted on the custom motion simulator. Periodic motion along the x-axis linear slide was achieved by the stepper motor via a belt. The natural arc of radioulnar motion was possible due to a second, free-moving, z-axis, linear slide

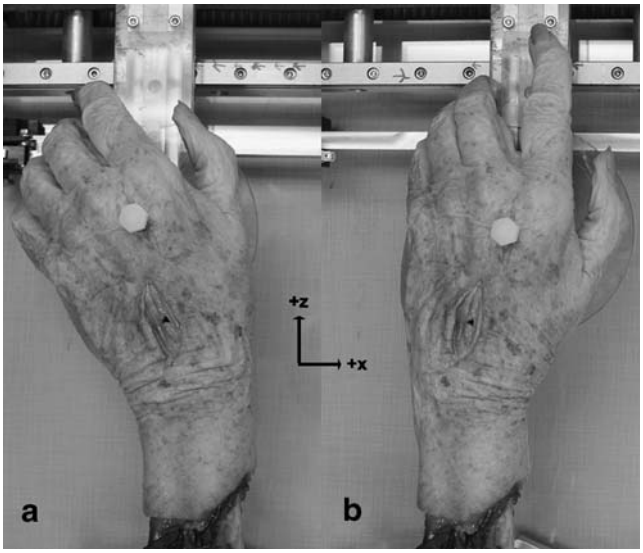

Fig. 2 The figure shows the extent of radioulnar deviation achieved by the cadaveric left wrist while on the motion simulator. **a** The wrist in full ulnar deviation (20°), and **b** the wrist in full radial deviation (10°)

Materials and methods

The study was approved by the institutional review board, orthopedic research review committee, and the radiology research review committee.

Motion simulator

A fresh frozen cadaveric forearm amputated from just below the elbow was used for the study. The proximal ends of the radius and ulna bone were exposed and firmly mounted onto a custom-made motion simulator (Fig. 1). The hand was mounted onto an acrylic paddle via a single plastic screw through the second intermetacarpal space just proximal to the deep intermetacarpal ligament. Two linear slides (the longer one oriented along the x-axis and the shorter one along the z-axis) under the paddle allowed it to have composite motions in the x and z-axes. A programmable Si5580 step motor drive and driver (Applied Motion Products, Watsonville, CA, USA) produced belt-driven

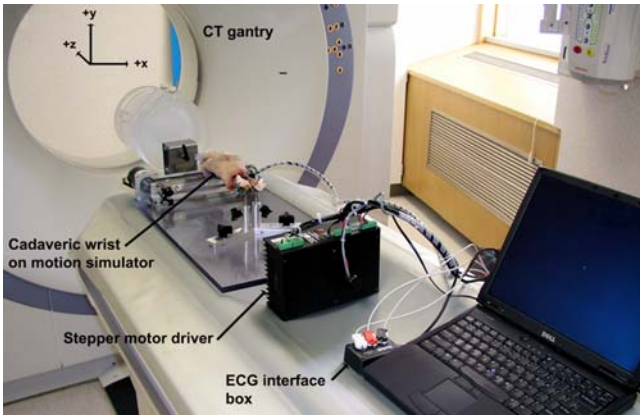

Fig. 3 The setup used for 4D CT wrist imaging

motion of the paddle in the x-axis, with free motion of the paddle in the z-axis allowing the hand to perform periodic (repeatable from cycle to cycle) radioulnar motion through a maximum arc of 30° (10° of radial deviation and 20° of ulnar deviation) (Fig. 2). An electronic trigger within the program, Si Programmer V2.5.7, produced a periodic 10 ms voltage spike linked to the motion profile of the stepper motor. This spike was detected by the CT scanner via an ECG interface box for use with the retrospectively-gated CT reconstruction [30].

Gated CT scanning

The periodically moving wrist was scanned on a 64-slice CT scanner (Sensation 64, Siemens Medical Solutions, Forchheim, Germany) (Fig. 3) using a retrospectively-gated CT protocol with a special low pitch of 0.1 provided by the manufacturer. Such a low pitch value was necessary for scanning of the periodic wrist motion with a low enough frequency to minimize the velocity of the wrist [29]. As the range of the joint motion was fixed, the maximum velocity during each motion cycle was smaller for the lower frequency. Since the ECG detection algorithm in the Sensation 64 scanner would not allow an ECG rate of fewer than 27 cycles per minute, a motion frequency of 30 cycles per minute was used, allowing for a margin of tolerance.

Scanning was done with a 120 kVp, 150 mAs, 0.33 s gantry rotation time and 32x0.6 mm detector collimation with z-flying focal spot [31, 32]. Use of a cardiac reconstruction algorithm allowed the temporal resolution of 165 ms.

Dynamic (four-dimensional) and static (three-dimensional) conditions

Scanning was performed from the distal radius and ulna to the proximal metacarpals to ensure adequate coverage of the carpal bones. The cadaveric wrist was scanned under dynamic and static conditions. Scanning under dynamic condition was performed during periodic radioulnar motion, with the wrist moving from radial deviation to ulnar deviation in a repeatable cyclic manner. This condition was designated the 4D condition. The static condition served as a control. In that condition, the wrist was moved precisely to four designated static positions (20° ulnar deviation, 10° ulnar deviation, 0°, and 10° radial deviation) and scanned in each of these positions. This condition was designated three-dimensional (3D) condition. In our cadaveric specimen, 20° of ulnar deviation (UD) and 10° of radial deviation (RD) corresponded to the extremes of radioulnar deviation.

Image reconstruction

Each data set was reconstructed with slice widths of 0.6 mm, a 150 mm field of view (FOV), and a sharp reconstruction kernel of B70f. The voxel size was 0.29x 0.29x0.6 mm^3.

Four different phases of the motion cycle from the 4D condition were selected for comparisons with the 3D condition. These phases corresponded to wrist positions of 20° ulnar deviation (phase 1), 10° ulnar deviation (phase 2), 0° (phase 3), and 10° radial deviation (phase 4).

Image analysis

The DICOM CT data were imported into Analyze 7.0 (Mayo Foundation for Medical Education and Research, MN, USA) for image analysis. The four phases of the motion cycle were evaluated for overall image quality and

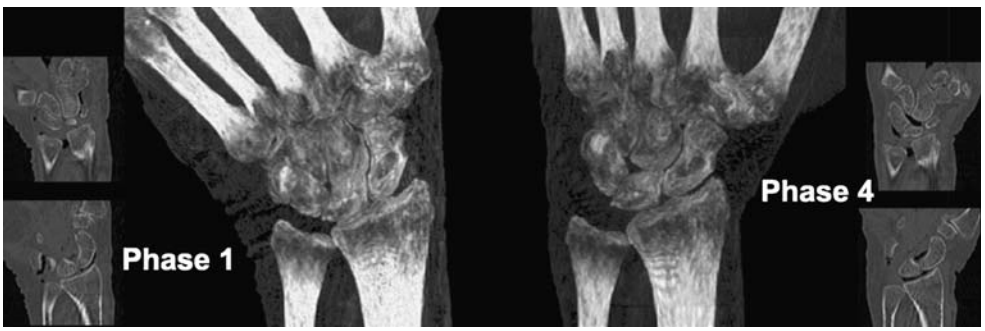

Fig. 4 The 4D condition at phase 1 and phase 4. There are no artifacts seen in either phase, and carpal joint spaces are well resolved, as can be seen in the coronal images (*inset*)

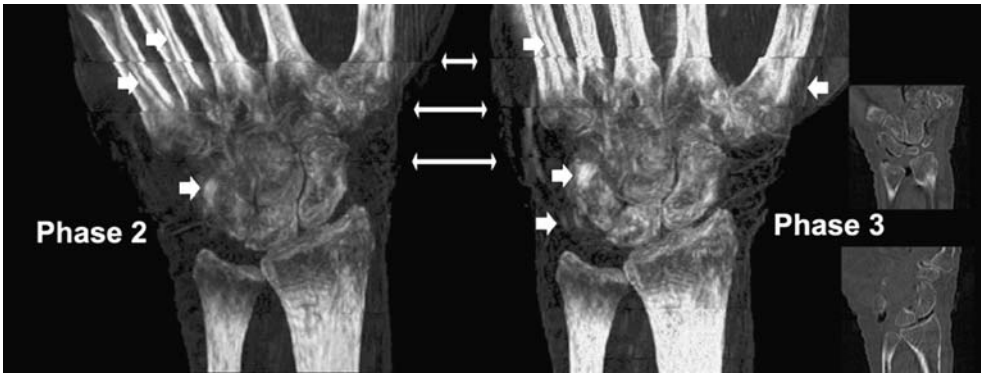

Fig. 5 The 4D condition showing phases 2 and 3. The image quality here is not ideal. Motion artifacts (*broad arrows*) can be seen. They are particularly prominent in the metacarpal region, but they are also present in the proximal carpal row. Band artifacts (*double-headed arrows*) are also seen. In the metacarpal region; displacements in band artifacts can also be seen, as shown by the presence of cortical mismatch in the metacarpals

for the presence of motion artifacts. A subjective scale of 1 to 4 (1 = excellent, 2 = good, 3 = fair, and 4 = poor) was used to grade the overall image quality by two independent blinded raters—a hand surgeon and a radiologist.

The displacement at the distal pole of the scaphoid was also calculated during radioulnar deviation using image registration methods. This was achieved by performing automatic surface registration of the scaphoid at phase 4 (10° of radial deviation) and at phase 1 (20° of ulnar deviation) after appropriate segmentation and thresholding of the scaphoid. After we had digitized the most distal point of the scaphoid from phase 4, a custom MATLAB 7.0.4 (The Mathworks, Natick, MA, USA) program calculated the magnitude of the displacement of the distal scaphoid.

Results

Image quality and artifacts

For the 4D images, both raters gave excellent scores for phases 1 and 4 (Fig. 4). Both raters gave fair scores to phases 2 and 3, although carpal joint spaces could still be resolved (Fig. 5). The image quality of the 3D condition was consistently graded as excellent for all four static positions assessed (Fig. 6).

The image quality degradation in phases 2 and 3 of the 4D images was due to artifacts (Fig. 5). Two main forms of artifacts were band artifacts [33] and motion artifacts [34, 35]. As can be seen, motion artifacts were particularly prominent in the metacarpals, which underwent higher motion velocity than did the carpal bones, as the metacarpals are situated further from the axis of rotation of the wrist [36]. The band artifacts are prominent in the metacarpal region too, as can be seen by the mismatching of the cortices of the metacarpal bones. This is mentioned, although our primary region of interest was the carpal bones. The images in the 4D condition in phases 1 and 4, on the other hand, were completely free of artifacts and were comparable to the images in the 3D condition (Figs. 4 and 5).

Distal scaphoid displacement

The distal scaphoid underwent a total displacement magnitude of 12.4 mm from phase 1 to 4 (20° ulnar deviation to 10° radial deviation). This was the displacement measured for a point on the distal scaphoid when it moved (under dynamic conditions) in 3D space from its position during radial deviation to ulnar deviation.

Discussion

The advent of 64-slice CT scanners with retrospective ECG-gating technology has provided a means for us to develop 4D (real-time dynamic) imaging of the wrist,

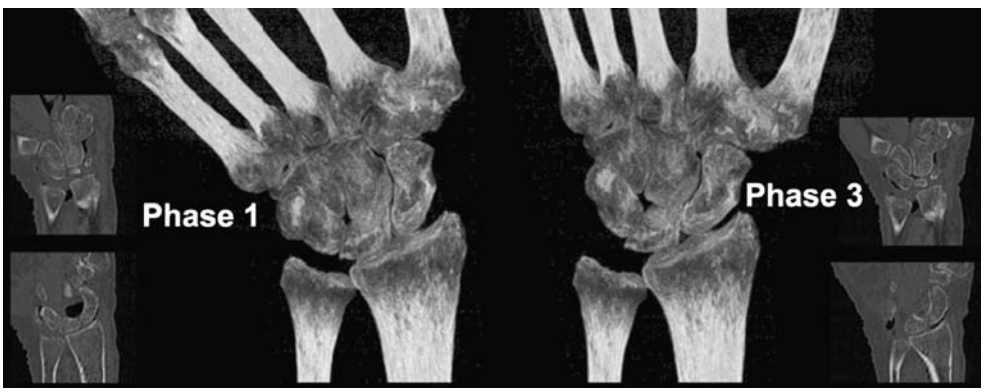

Fig. 6 The image quality from the 3D condition. As expected, there are no motion artifacts and carpal joint spaces are well resolved. Note that the end-motion phases (phases 1 and 4) of the 4D condition are of equivalent image quality to the 3D condition images

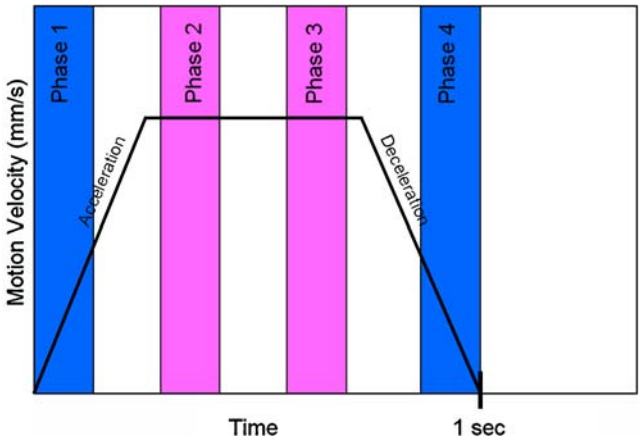

Fig. 7 The velocity motion profile of the stepper motor during one half-cycle of periodic motion. One half-cycle of periodic motion in this case would mean the movement of the wrist from full ulnar deviation to full radial deviation. The approximate locations of the analyzed phases of the motion cycle are as shown. The *pink phases* (phases 2 and 3) are the mid-motion phases, and the *blue phases* (phases 1 and 4) are the end-motion phases

which has the potential of providing more accurate diagnosis and assessment of dynamic carpal instabilities than dynamic fluoroscopy provides. With a temporal resolution as good as 83 ms, these CT scanners have the capability to capture real-time images, provided that the velocity of motion is not too fast [29].

If high-quality 4D imaging using retrospectively-gated CT technology is to be achieved, musculoskeletal motion must fulfill two criteria. It has to be periodic (repeatable from cycle to cycle), and the motion velocity should be kept as low as possible for the best image quality. Prior work has demonstrated that high-contrast spatial resolution of 0.8 mm with satisfactory image quality can be achieved when motion velocity is kept below 20 mm/s [29]. The 30 cycles per minute (cpm) frequency for periodic motion would likely be comfortably achieved in future in vivo applications with the aid of a special device that would allow precise control of wrist motion in human subjects.

The velocity motion profile of the stepper motor during one half-cycle of periodic motion is shown in Fig. 7. Phases 1 and 4, which were imaged at the extremes of motion (end-motion) had lower instantaneous motion velocity than did the mid-motion phases 2 and 3 and would be most appropriate for detailed analysis. This is analogous to the situation in cardiac imaging, where only the best phase images are used for assessment of coronary artery stenosis [1, 37]. We also noted that image quality tended to be worse in the metacarpals than in the carpal region, with more artifacts present. This was again due to the fact that the metacarpals, being further away from the axis of rotation [36], had a higher instantaneous motion velocity than the carpal bones had. Our estimates showed that the distal metacarpals moved at an approximate average velocity of 50 mm/s, while the average velocity at the distal scaphoid was only 12.4 mm/s.

Band artifacts are expected in gated CT scanning [33] when motion is not perfectly periodic or not ideally synchronized to the CT acquisition. These were not particularly bothersome, except when displacements occurred between the bands, resulting in cortical mismatches, as seen in the metacarpals. The severity of band artifact displacement was worsened with higher motion velocity. Thus, we saw band artifact displacements in the metacarpal regions. The magnitude of these artifacts can be reduced if one makes sure that the wrist cyclic motion is in perfect synchrony with the "ECG" signal recorded by the scanner. The remaining band artifacts can be corrected by retrospective editing of the "ECG" signal, provided that a clear object contour is visible in the image to assist with realignment (Fig. 8). We would like to point out that, although band artifacts compromise the overall image quality, they do not add to the degradation of the spatial resolution, which depends only on the motion velocity of the wrist.

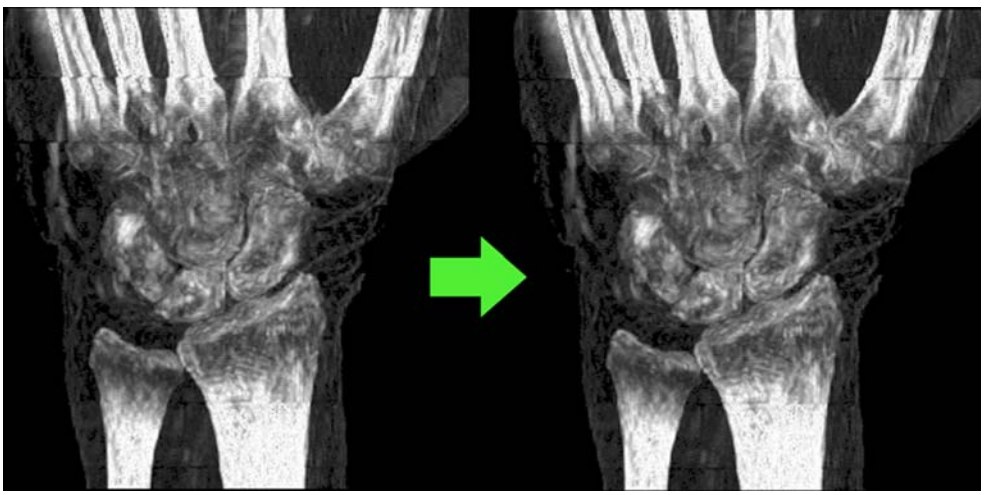

Fig. 8 This figure shows how band artifact displacement can be corrected by retrospective editing of the ECG signal. One can see that cortical mismatching is minimized in the image on the right. However, motion artifacts cannot be fixed in this manner and require either slower motion velocity or faster temporal resolution

Table 1 Features of 4D gated computed tomography (CT) using a 64-slice scanner versus 4D multi-projection II

Four-dimensional gated CT	Four-dimensional multi-projection II
High spatial resolution (0.8 mm)	Lower spatial resolution (1.5 mm)
Fast examination time (15 s)	Long examination time (80 s)
Few motion cycles needed (5)	Many motion cycles needed (50)
Time synchronization automated	Time synchronization manual
Relatively slow temporal resolution (165 ms)[a]	Fast temporal resolution (12 ms)
Artifacts in mid-motion phases	No artifacts
Requires periodic motion	Requires periodic motion

[a] 83 ms for the dual-source CT scanner (Siemens Definition)

Radiation dose is directly related to the effective milliamp-seconds (mAs/pitch). In our feasibility study, we used an effective mAs value of 1,500. This is approximately twice as high as that currently used in coronary CT angiography. However, as the wrist's X-ray attenuation is small, we should be able to reduce the effective milliamp-second value substantially without any significant loss in image quality. In addition, the wrist is not a radiation-sensitive body part, so the effective dose delivered during such an examination will be essentially zero.

Though we were not able to demonstrate excellent image quality in all phases of the motion cycle using gated CT scanning, the availability of high-quality images in the end-motion phases is still valuable for kinematics analysis of the extremes of joint motion. As we mentioned above, the end-motion dynamic images might provide useful information about dynamic wrist instabilities, which cannot be obtained by static imaging. As CT technology advances, image quality in the mid-motion phases will also improve, increasing the clinical value of this novel 4D MSK imaging technique. With the advent of dual-source CT scanners with even faster temporal resolution (83 ms) [38], motion artifacts will decrease, while the use of wider detectors (e.g., the new 256-slice Toshiba with 12.8 cm detector width) will reduce or eliminate band artifacts, because fewer motion cycles will be needed to cover the joint region.

Gated spiral CT is not the only way to achieve 4D imaging of the wrist. Carelsen et al [25] have also developed a novel method, using multi-projection image intensifiers (II) to image periodic wrist motion. Their method does not suffer from motion artifacts, due to the fast temporal resolution of the image intensifiers (12 ms). However, it has poorer spatial resolution, owing to the low number of projections used to reconstruct a 3D image, and it requires a prolonged examination time of 80 s, as a minimum of 50 wrist motion cycles is needed. This large number of repetitions may be a problem if the patient is suffering from significant wrist pain. The main limiting factor of the gated CT technique is its temporal resolution resulting in motion artifacts in the mid-motion phases (Table 1) [35, 39]. A real advantage of the dynamic CT approach is its capability to produce high-quality multiplanar reconstruction (MPR) images of various phases of wrist motion, due to the isotropic spatial resolution of modern multi-detector row CT scanners.

In conclusion, our preliminary testing of a novel gated CT scanning technique for the wrist has shown that it is feasible and provides most information in end-motion phases, which we recognize would currently limit its clinical value. We anticipate that advances in CT technology, such as faster temporal resolution and wider detector coverage, will, in the near future, further improve dynamic wrist imaging by overcoming the limitations identified in our preliminary work. We believe we have demonstrated the feasibility of a novel technique with clinical potential in the diagnosis and assessment of wrist instabilities.

Acknowledgments Dr. Tay wishes to acknowledge financial support from Mayo Foundation, Rochester, MN, USA and National Medical Research Council, Singapore. The authors would like to thank Mr. Larry Berglund for the construction of the motion simulator and Ms Kristina Nunez for assistance with manuscript preparation.

References

1. Achenbach S, Ropers D, Kuettner A, et al. Contrast-enhanced coronary artery visualization by dual-source computed tomography—initial experience. Eur J Radiol 2006; 57: 331–335.
2. Kopp AF, Ohnesorge B, Flohr T, et al. [Cardiac multidetector-row CT: first clinical results of retrospectively ECG-gated spiral with optimized temporal and spatial resolution]. Rofo Fortschr Geb Rontgenstr Neuen BildgebVerfahr 2000; 172: 429–435.
3. Nikolaou K, Flohr T, Knez A, et al. Advances in cardiac CT imaging: 64-slice scanner. Int J Cardiovasc Imaging 2004; 20: 535–540.
4. Dewey M, Laule M, Krug L, et al. Multisegment and halfscan reconstruction of 16-slice computed tomography for detection of coronary artery stenoses. Invest Radiol 2004; 39: 223–229.
5. Dewey M, Muller M, Teige F, et al. Multisegment and halfscan reconstruction of 16-slice computed tomography for assessment of regional and global left ventricular myocardial function. Invest Radiol 2006; 41: 400–409.
6. Dewey M, Rutsch W, Schnapauff D, Teige F Hamm B. Coronary artery stenosis quantification using multislice computed tomography. Invest Radiol 2007; 42: 78–84.
7. Keall PJ, Starkschall G, Shukla H, et al. Acquiring 4D thoracic CT scans using a multislice helical method. Phys Med Biol 2004; 49: 2053–2067.
8. Nehmeh SA, Erdi YE, Pan T, et al. Four-dimensional (4D) PET/CT imaging of the thorax. Med Phys 2004; 31: 3179–3186.
9. Pan T, Lee TY, Rietzel E, Chen GT. 4D-CT imaging of a volume influenced by respiratory motion on multi-slice CT. Med Phys 2004; 31: 333–340.
10. Elgeti T, Proquitte H, Rogalla NE, et al. Evaluation of a reduced dose protocol for respiratory gated lung computed tomography in an animal model. Invest Radiol 2007; 42: 230–234.

11. Berdia S, Short WH, Werner FW, Green JK, Panjabi M. The hysteresis effect in carpal kinematics. J Hand Surg [Am] 2006; 31: 594 e1–594 e8.
12. Short WH, Werner FW, Fortino MD, Mann KA. Analysis of the kinematics of the scaphoid and lunate in the intact wrist joint. Hand Clin 1997; 13: 93–108.
13. Bachofen H, Hildebrandt J. Area analysis of pressure-volume hysteresis in mammalian lungs. J Appl Physiol 1971; 30: 493–497.
14. Watson H, Ottoni L, Pitts EC, Handal AG. Rotary subluxation of the scaphoid: a spectrum of instability. J Hand Surg [Br] 1993; 18: 62–64.
15. Werner FW, Short WH, Green JK. Changes in patterns of scaphoid and lunate motion during functional arcs of wrist motion induced by ligament division. J Hand Surg [Am] 2005; 30: 1156–1160.
16. Teoh LC, Yam AK. Anatomic reconstruction of the distal radioulnar ligaments: long-term results. J Hand Surg [Br] 2005; 30: 185–193.
17. Adams BD, Berger RA. An anatomic reconstruction of the distal radioulnar ligaments for posttraumatic distal radioulnar joint instability. J Hand Surg [Am] 2002; 27: 243–251.
18. Bickert B, Sauerbier M, Germann G. Scapholunate ligament repair using the Mitek bone anchor. J Hand Surg [Br] 2000; 25: 188–192.
19. Walsh JJ, Berger RA, Cooney WP. Current status of scapholunate interosseous ligament injuries. J Am Acad Orthop Surg 2002; 10: 32–42.
20. Wolf JM, Weiss AP. Bone-retinaculum-bone reconstruction of scapholunate ligament injuries. Orthop Clin North Am 2001; 32: 241–246, viii.
21. Darlis NA, Weiser RW, Sotereanos DG. Partial scapholunate ligament injuries treated with arthroscopic debridement and thermal shrinkage. J Hand Surg [Am] 2005; 30: 908–914.
22. Watson HK, Weinzweig J, Zeppieri J. The natural progression of scaphoid instability. Hand Clin 1997; 13: 39–49.
23. Berger RA. The anatomy and basic biomechanics of the wrist joint. J Hand Ther 1996; 9: 84–93.
24. Camus EJ, Millot F, Lariviere J, Raoult S, Rtaimate M. Kinematics of the wrist using 2D and 3D analysis: biomechanical and clinical deductions. Surg Radiol Anat 2004; 26: 399–410.
25. Carelsen B, Bakker NH, Strackee SD, et al. 4D rotational X-ray imaging of wrist joint dynamic motion. Med Phys 2005; 32: 2771–2776.
26. Crisco JJ, Coburn JC, Moore DC, Akelman E, Weiss AP, Wolfe SW. In vivo radiocarpal kinematics and the dart thrower's motion. J Bone Joint Surg Am 2005; 87: 2729–2740.
27. Kobayashi M, Berger RA, Nagy L, et al. Normal kinematics of carpal bones: a three-dimensional analysis of carpal bone motion relative to the radius. J Biomech 1997; 30: 787–793.
28. Shim SS, Kim Y, Lim SM. Improvement of image quality with beta-blocker premedication on ECG-gated 16-MDCT coronary angiography. AJR Am J Roentgenol 2005; 184: 649–654.
29. Tay S, Primak A, Fletcher J, Schmidt B, An KN, McCollough CH. Understanding the relationship of image quality to motion velocity in gated-CT imaging: preliminary work for 4D musculoskeletal imaging. J Comput Assist Tomogr 2007 (in press).
30. Ohnesorge B, Flohr T, Becker C, et al. Cardiac imaging by means of electrocardiographically gated multisection spiral CT: initial experience. Radiology 2000; 217: 564–571.
31. Kyriakou Y, Kachelriebeta M, Knaup M, Krause JU, Kalender WA. Impact of the z-flying focal spot on resolution and artifact behavior for a 64-slice spiral CT scanner. Eur Radiol 2006; 16: 1206–1215.
32. Flohr T, Stierstorfer K, Raupach R, Ulzheimer S, Bruder H. Performance evaluation of a 64-slice CT system with z-flying focal spot. Rofo Fortschr Geb Rontgenstr Neuen BildgebVerfahr 2004; 176: 1803–1810.
33. Taguchi K, Chiang BS, Hein IA. Direct cone-beam cardiac reconstruction algorithm with cardiac banding artifact correction. Med Phys 2006; 33: 521–539.
34. McCollough CH, Bruesewitz MR, Daly TR, Zink FE. Motion artifacts in subsecond conventional CT and electron-beam CT: pictorial demonstration of temporal resolution. Radiographics 2000; 20: 1675–1681.
35. Mori S, Endo M, Asakura H. Improvement in banding artefacts in four-dimensional computed tomography for radiotherapy planning. Phys Med Biol 2006; 51: 5231–5244.
36. Kaufmann R, Pfaeffle J, Blankenhorn B, Stabile K, Robertson D, Goitz R. Kinematics of the midcarpal and radiocarpal joints in radioulnar deviation: an in vitro study. J Hand Surg [Am] 2005; 30: 937–942.
37. Greuter MJ, Dorgelo J, Tukker WG, Oudkerk M. Study on motion artifacts in coronary arteries with an anthropomorphic moving heart phantom on an ECG-gated multidetector computed tomography unit. Eur Radiol 2005; 15: 995–1007.
38. Flohr TG, McCollough CH, Bruder H, et al. First performance evaluation of a dual-source CT (DSCT) system. Eur Radiol 2006; 16: 256–68.
39. Taguchi K. Temporal resolution the evaluation of candidate algorithms for four-dimensional CT. Med Phys 2003; 30: 640–650.